

Passive Daytime Cooling Foils for Everyone: A Scalable Lamination Process Based on Upcycling Aluminum-Coated Chips Bags

Qimeng Song* and Markus Retsch*

Cite This: *ACS Sustainable Chem. Eng.* 2023, 11, 10631–10639

Read Online

ACCESS |



Metrics & More



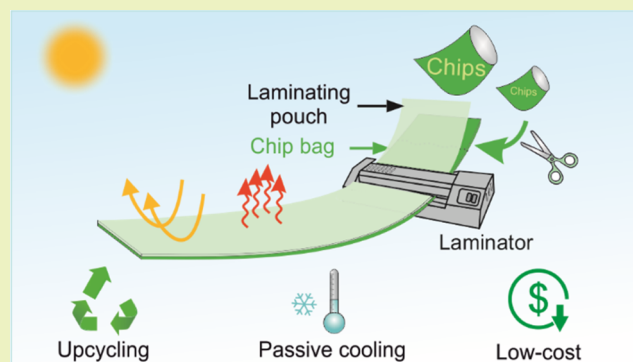
Article Recommendations



Supporting Information

ABSTRACT: The increasing energy demand for space cooling and environmental pollution caused by post-consumer plastic waste are two of the most challenging issues today. Passive daytime cooling, which dissipates heat to outer space without external energy input, has emerged recently as a sustainable technique for space cooling. In this work, a plastic waste-based passive daytime cooling foil is reported to alleviate both issues simultaneously. The mirror-like aluminum-plastic laminate (APL) waste exhibits a satisfactory solar reflectance of 85.7%. Combining the APL waste with a laminated pouch foil reveals a remarkably simple but effective plastic waste-based cooling foil with a high emissivity of 0.87 in the atmospheric window, resulting in a compelling daytime cooling performance. The sustainable aluminum-plastic laminate waste-based cooling foil is flexible, easily scalable, low-cost, and fabricated with a common laminator. This makes the fabrication of passive cooling materials possible even for nonexperts, which will help to provide advanced sun shelters and comfortable temperatures to a wider community.

KEYWORDS: plastic waste upcycling, radiative cooling, heat management, laminated pouch, thermal comfort



INTRODUCTION

Plastics have become the most indispensable materials in our daily lives. It was reported that global plastic production reached about 370 million tons in 2019.¹ Plastic products bring us convenience while causing severe environmental issues.² Despite the utmost effort that has been made, only 9% of the plastic post-consumer waste is recycled.³ Among all of the various sorts of plastic post-consumer waste, aluminum-plastic laminate (APL) is one of the most challenging ones to recycle.^{4,5} APL, a layer of aluminum laminated with multiple polymer layers, is a popular material in a range of product packaging, such as snack food, coffee beans, and pharmaceutical products. With an aluminum (Al) barrier layer blocking the moisture, light, and gas, the shelf time of the products are greatly elongated. However, the multilayer composition of APL makes it extremely difficult to recycle. Thus, it is still considered a nonrecyclable material.⁶ To increase the recycling rate of the post-customer APL waste, various strategies have been invented, such as chemical and thermal delamination^{7,8} and enzymatic bioleaching.⁹ Still, a significant portion of APL waste is discarded in landfills or treated by incineration, with adverse effects such as soil infertility, air pollution, and greenhouse gas emission,^{10,11} and causes threats to the natural environment, wildlife, and ultimately to human beings. Therefore, a more cost-efficient recycling strategy or repurposing of APL is urgently desired.

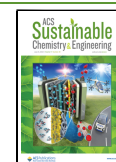
Passive daytime cooling is a newly emerging technique that dissipates heat from terrestrial objects to outer space through the

atmospheric window (8–13 μm) without external energy consumption.^{12–14} It is considered a promising contribution to the fight against urgent issues caused by the overuse of fossil fuels, such as global warming and extreme weather. This technique's core is to minimize the energy uptake from solar light and simultaneously maximize the heat release via thermal radiation to outer space (3K). Therefore, to achieve net passive cooling in the daytime under intense solar light, low absorption in the solar range and a high mid-infrared (MIR) emission are mandatory for a passive daytime cooling device. In the last few years, benefiting from the rapid development of micro- or nanotechnology in materials processing, an increasing number of cooling devices with superior optical properties have been revealed, including ultrawhite paint,^{15,16} nanophotonic devices,^{17,18} porous polymer films,^{19–21} and polymer–nanoparticle composites,^{22,23} achieving remarkable daytime subambient cooling performance. Although progress has been made, this zero-energy-input cooling technique has not transitioned into an end-user product available in our daily life. The main obstacle is its sophisticated fabrication process and scalability.

Received: February 4, 2023

Revised: June 23, 2023

Published: July 13, 2023



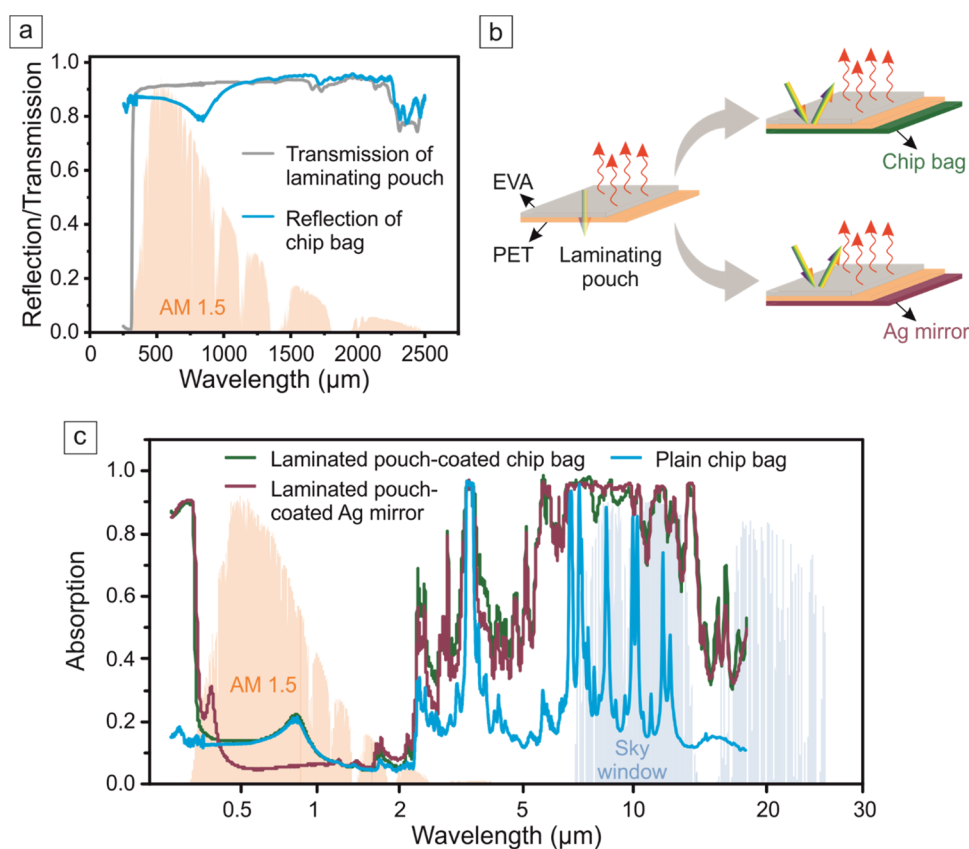


Figure 1. (a) Solar reflection and transmission of a plain chip bag and laminated pouch foil, respectively. (b) Schematic shows the concept of passive daytime cooling with a laminated pouch-based cooling device. (c) Optical property of a laminated pouch ($\sim 80 \mu\text{m}$)-covered chip bag and Ag mirror. The AM 1.5 solar intensity spectrum (highlighted in orange) and atmospheric transparency window (highlighted in blue) were plotted as the background.

Apart from the advanced cooling devices fabricated with the sophisticated process, a simple cooling device can be constructed with metal mirror-backed emitters, such as the poly(dimethylsiloxane) (PDMS)-coated silver (Ag) or aluminum mirror.^{24,25} APL waste demonstrates a mirror-like appearance because of the Al layer in the laminate, which endows it with great potential in the application of daytime solar reflection. In this work, we report a practical strategy to convert APL packaging waste to high-value foils with passive daytime cooling properties. By coupling the APL waste with a laminated pouch via a common hot laminator, we fabricated a simple, sustainable, and effective passive daytime cooling foil, which exhibits a satisfactory solar reflectance of 85.7% and mid-infrared thermal emittance of 0.87, thus achieving an attractive passive cooling performance. The foreseeable scalable and low-cost cooling foil proposed here paves the way for mass production of this zero-emission cooling technique. Additionally, the fabrication process is fairly easy to be carried out, even by nonexperts. By spreading this technique worldwide, we believe that every household can fabricate their own passive daytime cooling foil, comforting them in hot climates while contributing to alleviating global warming and greenhouse gas emissions.

EXPERIMENTAL SECTION

Materials. Laminating pouch foils (A4, glossy) with different thicknesses, i.e., 80, 100, 125, and 250 μm , were purchased from General Binding Corporation (GBC) and used as received. A Ag mirror with a thickness of 3.2 mm (dia. = 5 cm) was obtained from Thorlabs.

Fabrication of APL Waste-Based Cooling Foils. For the Laminated Pouch on the Mirror. Laminating pouch foil of identical size to the mirror was attached to the Ag mirror by a hot-pressing technique on a hot plate with a temperature of 90 $^{\circ}\text{C}$.

For the Laminated Pouch on the Chip Bag. Chip bags were collected from plastic waste and cleaned with standard detergent and adequate water. Subsequently, the chip bags were rinsed with ethanol and Milli-Q water and dry for later processing. The resulting chip bags were then placed between two laminating pouch foils and hot laminated using an office laminator (A350 Combo, OLYMPIA). All of the samples were cut to a size of dia. = 5 cm for indoor and rooftop measurements.

Scanning Electron Microscopy (SEM) and Optical Microscopy. SEM images of a laminating pouch foil cross-section were taken with a Zeiss Ultra plus (Carl Zeiss AG, Germany) at an operating voltage of 3 kV and with in-lens detection. Optical microscopy images of the laminating pouch foil cross-section were obtained with a three-dimensional (3D) laser scanning microscope (LEXT OLS 5000, Olympus).

Chemical Composition Determination. The chemical composition of the laminating pouch foil was determined by using Fourier-transform infrared spectroscopy (FTIR) spectroscopy (Vertex 70, Bruker) with attenuated total reflectance (ATR) mode for both sides. Absorption spectra were collected in the range of 7500–380 cm^{-1} with a spectral resolution of 4 cm^{-1} . 64 scans were averaged for each spectrum, and air was used for the background spectra.

Optical Property Characterization with UV–Vis and FTIR Spectroscopy. Solar reflectance was measured by using a UV–vis spectrometer (Cary 5000, Agilent Technologies) equipped with an integrating sphere accessory (Labspheres) with a fixed incident angle of 8 $^{\circ}$. A Spectralon diffuse reflectance standard (Labspheres) was applied as the reference. The optical property of samples in the MIR regime was determined with an FTIR spectroscope (Vertex 70, Bruker) equipped

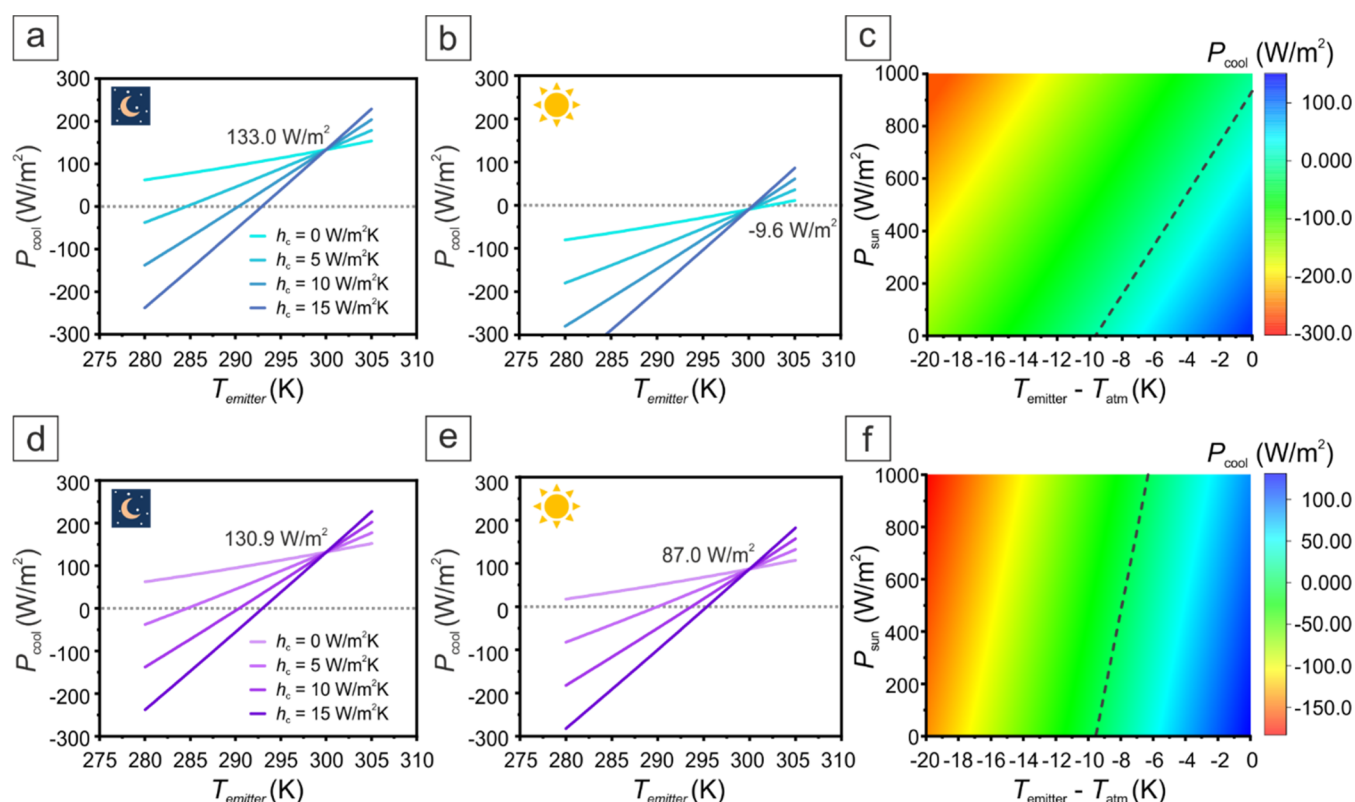


Figure 2. Predicted net cooling power for a laminated pouch-coated (a, b) chip bag and (d, e) Ag mirror with various nonradiative heat transfer coefficients (h_c), 0, 5, 10, 15 $\text{W}/(\text{m}^2 \text{K})$. The AM 1.5 solar spectrum with a power intensity of $1000 \text{ W}/\text{m}^2$ is used for daytime calculations. Predicted net cooling power as a function of solar intensity and temperature difference between the emitter and ambient for a laminated pouch-coated (c) chip bag and (f) Ag mirror, with $h_c = 10 \text{ W}/(\text{m}^2 \text{K})$. Dashed lines indicate zero net cooling power. An ambient temperature of 300 K was used for all numerical calculations.

with a gold-coated integrating sphere accessory (A562, Bruker). A gold mirror was applied as the reference. The absorptance (emittance) was calculated with absorptance (emittance) = $1 - \text{reflectance}$. Transmission is assumed to be neglectable due to the presence of the Al layer or Ag layer.

Indoor Measurement for Cooling Performance Characterization. For all indoor measurements, dried air was warmed by a water bath to $40 \text{ }^\circ\text{C}$ and flushed in the area between the convection shield and measurement cell with a volumetric flow rate of $80 \text{ l}_v/\text{min}$. The Al dome was cooled with liquid nitrogen down to about $-190 \text{ }^\circ\text{C}$. Before filling the liquid nitrogen into the setup, the inner space of the dome was flushed with nitrogen to avoid water condensation. The temperature of the dome was maintained constant during the entire measurement by continuously filling liquid nitrogen into the setup. A thermocouple (type T) was used for recording the temperature, and data was collected by a digital multimeter (DAQ6510, Tektronix, Germany) every 5 s.

For the measurements with different solar intensities, AM 1.5 solar light was provided by a solar simulator (AX-LAN400, SCIENCE-TECH, CANADA) with an illumination area of $5 \times 5 \text{ cm}^2$. The solar intensity was changed stepwise from 0 to 25, 50, 75, and 100% of one sun ($\sim 1000 \text{ W}/\text{m}^2$) after the sample temperature reached a steady state.

Rooftop Measurement for Cooling Performance Characterization. Rooftop measurements for laminated pouch-based cooling devices were carried out on the roof of a four-floor building (August 3rd, 2022, University of Bayreuth, Bayreuth, Germany) under a clear sky. All of the test samples were placed in identical homemade sample holders. The holders were thermally insulated by styrofoam and covered with aluminum foil. A low-density polyethylene (LDPE) foil with a thickness of about $15 \text{ }\mu\text{m}$ is applied to block convective heat transfer. The temperatures of the samples were determined by Pt-100 temperature sensors and recorded with a digital multimeter (DAQ6510, Tektronix, Germany) every 5 s. The ambient temperature

was recorded by a thermocouple enclosed in a similar styrofoam box, the top and bottom of which are covered by LDPE to block the convection but allow solar transmission. The solar irradiance data were collected from the weather station at the University Bayreuth (Ecological-Botanical Garden, 400 m away from the rooftop measurement). The relative humidity (RH) was tracked with a temperature logger (LOG220, DOSTMANN electronic GmbH) next to the measurement setup. The absolute humidity (AH) in g/m^3 was calculated using RH and ambient temperature (T_{amb}) by

$$\text{AH} = \frac{6.112 \cdot \exp\left(\frac{17.67 \cdot T_{\text{amb}}}{T_{\text{amb}} + 243.5}\right) \cdot \text{RH} \cdot 2.1674}{273.15 + T_{\text{amb}}}$$

For field testing with umbrellas, two umbrellas, one covered with laminated pouch-coated chips, were placed on the roof of a four-floor building (August 11th, 2022, University of Bayreuth, Bayreuth, Germany) under a clear sky. Infrared thermal images were taken by using an IR camera (VarioCAMHD, Jenoptik). The temperature of the umbrellas was measured by a thermocouple (type T) attached to the umbrella's inner side and recorded with a digital multimeter (DAQ6510, Tektronix, Germany) every 5 s.

RESULTS AND DISCUSSION

Fabrication and Characterization of the APL Waste-Based Cooling Foil. The optical property of a typical APL packaging, i.e., the chip bag, was characterized in the solar range. Figure 1a shows the solar reflection spectrum of a chip bag. A solar reflection, up to 86%, is observed from the side facing inside, arising from the presence of the Al layer. To achieve net cooling performance, efficient radiative heat release associated with high emissivity over the atmospheric window range is mandatory. Most plain APLs do not possess high emissivity, restricted by the inherent polymer in the laminate and the

limited layer thickness.²⁶ Laminated pouches are common household items. The pouch consists of a poly(ethylene terephthalate) (PET) polymer film coated with an ethylene-vinyl acetate (EVA) thermoadhesive layer on one side. By applying heat and pressure using a roll-to-roll thermal laminator, the pouch will strongly bond to the material that needs to be protected. With optical and scanning electron microscopy (SEM), we can clearly see the two-layer structure of the pouch foil (Figure S1). The chemical composition of the EVA and PET sides of a laminated pouch was confirmed by Fourier-transform infrared spectroscopy (FTIR) measurements with an ATR mode. The absorption spectra for both sides are illustrated in Figure S2a. The EVA side shows absorption peaks at 2848–2916, 1735, 1465, and 1020–1238 cm^{-1} , which are assigned to the C–H stretching vibrations, C=O stretching vibrations, C–H (in CH_2 and CH_3) antisymmetric deforming and stretching vibrations of C–O (in $=\text{C}-\text{O}-\text{C}$), respectively.²⁷ Similar to EVA, the stretching vibrations of C=O and C–O (in $=\text{C}-\text{O}-\text{C}$) of PET cause the absorption peak at 1713 and 1018–1245 cm^{-1} , respectively. Besides, peaks at 1506, 872, and 723 cm^{-1} were also obtained on the PET side, which are attributed to the stretching vibration of C=C (in the aromatic ring), 1,2,4,5-tetrasubstituted aromatic rings, and the interaction of polar ester groups and benzene rings, respectively.²⁸ Thanks to the specific absorption peak contributed by the molecular band vibrations of PET and EVA, laminated pouch foil exhibit remarkable selective MIR emissivity in the atmospheric window range (8–13 μm , Figure S2b). An average emissivity, weighted by the black-body spectrum, of 0.87 is obtained. In addition, the laminated pouch possesses a marked transmittance in the solar range, which is indicated by the UV/vis spectra shown in Figure 1. The superior optical properties in both solar and MIR ranges make the laminated pouch an outstanding candidate as the MIR emission enhancer for APL to be an excellent passive daytime cooling foil. The concept of the laminating pouch and chip bag constructed passive daytime cooling foil is shown in Figure 1b. The highly selective emissivity of the pouch foil will ensure an effective heat release from the cooling foil to outer space via thermal radiation. At the same time, the chip bag will hinder the energy uptake from the solar light via reflecting for daytime application. To demonstrate this concept, we coated a chip bag with a commercial laminated pouch (thickness of $\sim 80 \mu\text{m}$) using an office laminator. We also coated the pouch on a highly solar-reflective Ag mirror as a reference substrate to emphasize the ability of the laminated pouch to serve as a promising emissive layer. The absorption spectrum for a plain chip bag, a laminated pouch-coated chip bag, and a Ag mirror is shown in Figure 1c. The laminated pouch coating greatly enhances the emissivity of the chip bag, while the solar absorption is negligibly influenced. A numerical calculation obtains an average solar absorption of 14.3% and an average emissivity of 0.87 with the laminated pouch-coated chip bag. In addition, the Ag mirror reflects most of the solar light, and an average solar absorption of 3.9% and an average emissivity of 0.87 is observed.

Numerical Calculations. To theoretically demonstrate the cooling performance of the laminated pouch-based cooling devices, we simplistically calculated the net cooling power based on the measured absorption spectra with a widely used radiative model (see the Supporting Information for the detailed calculation).¹⁴ The predicted net cooling power with various nonradiative heat transfer coefficients (h_c), i.e., 0, 5, 10, and 15 $\text{W}/(\text{m}^2 \text{K})$, is shown in Figure 2a,b,d,e for a laminated pouch-coated chip bag and Ag mirror, respectively. In the nighttime, a

net cooling power of about 130 W/m^2 can be expected for both cooling devices when the temperature of the cooling devices is equal to the ambient temperature. In the daytime, under the solar intensity of about 1000 W/m^2 , the energy absorbed by the laminated pouch-coated chip bag is observed to be slightly larger than what could be released, resulting in a small but negative net cooling power ($-9.6 \text{ W}/\text{m}^2$). By contrast, by reflecting most of the solar light, the laminated pouch-coated Ag mirror is obtained to show a net cooling power of 87.0 W/m^2 . In addition, when the cooling power equals zero, different subambient cooling can be reached by the laminated pouch-based cooling devices, depending on the h_c . For instance, with $h_c = 10 \text{ W}/(\text{m}^2 \text{K})$, a subambient cooling of 9.6 $^\circ\text{C}$ was predicted for both the laminated pouch-coated chip bag and Ag mirror in the nighttime. In the daytime, the laminated pouch-coated chip bag will be slightly heated (0.7 $^\circ\text{C}$) by the intensive solar light, and a subambient cooling of 5.3 $^\circ\text{C}$ can be expected with the laminated pouch-coated Ag mirror. Even though the laminated pouch-coated chip bag could not achieve a net cooling power with 1000 W/m^2 solar power intensity, it could afford an attractive cooling performance over 24 h, based on the fact that the solar intensity varies all day and barely exceeds 900 W/m^2 . To prove this point, we thus carried out the net cooling power simulation with varying solar intensity. A simulation result with $h_c = 10 \text{ W}/(\text{m}^2 \text{K})$ for a laminated pouch-coated chip bag and a Ag mirror is shown in Figure 2c,f. The simulations with more various h_c , i.e., 0, 5, 10, and 15 $\text{W}/(\text{m}^2 \text{K})$, can be found in Figures S3 and S4. From the numerical calculations, we can see that when the temperature is the same as the ambient temperature, the pouch-coated chip bag can provide net cooling power for most of the solar intensity range, which confirms its excellent cooling performance throughout the day. A positive net cooling power is observed up to a solar intensity of 933 W/m^2 .

In the market, pouch foil with various thicknesses is available for hot lamination application. The thickness of homogeneous polymer films influences not only the MIR absorption but also the absorption in the solar range. A comprehensive investigation of the impact of layer thickness on passive daytime cooling performance is reported in our previous work.²⁹ To reveal the optimized thickness for a maximized passive daytime cooling performance of laminated pouch-based cooling films, we determined the optical properties of market-accessible laminated pouches with various thicknesses, i.e., 80, 100, 125, and 250 μm . Figure S5 shows the absorption spectra over the UV/vis and MIR range of laminated pouch-coated chip bags and Ag mirrors with various pouch thicknesses. The absorption spectra show that with increasing the film thickness, the absorption in both solar and MIR range is gradually enhanced, agreeing with the simulation result observed in our previous work.²⁹ The average absorption in the solar and atmospheric window range was calculated based on the spectrum of AM 1.5 solar irradiation³⁰ and atmosphere transmission³¹ and plotted as a function of pouch thickness (Figure S6). The thickness increase of the laminated pouch foil from 80 to 250 μm increased the average solar absorption from 14.3 to 16.1% for the laminated pouch-coated chip bag and from 3.9 to 8.4% for the laminated pouch-coated Ag mirror. Simultaneously, it increased the MIR absorption from 0.87 to 0.92 for both structures. To further quantify the impact of the pouch foil thickness on the net cooling performance, we calculated the net cooling power of the laminated pouch-based cooling devices with various thicknesses based on the measured spectra. As shown in Figure S7, the

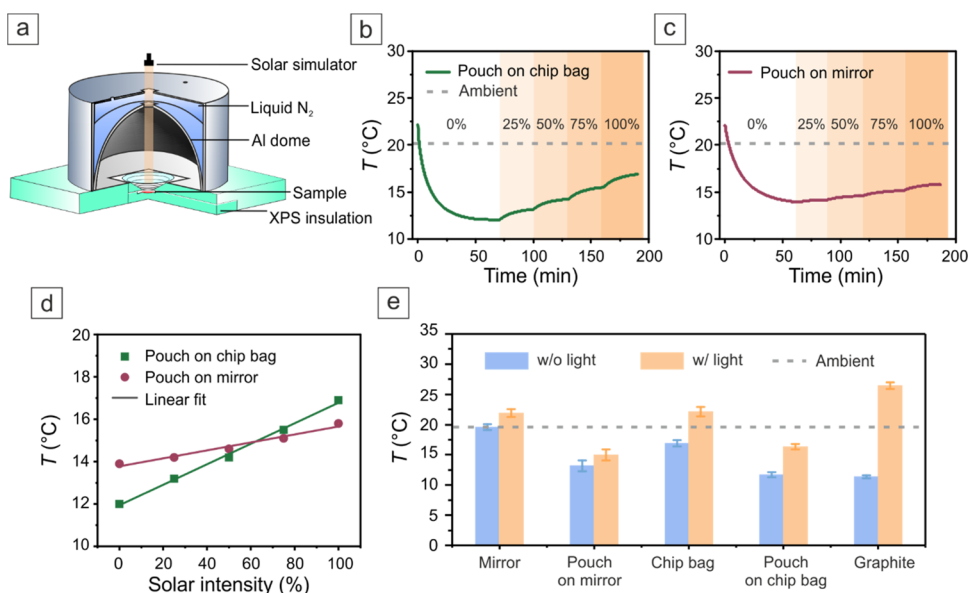


Figure 3. (a) Schematic of the setup for indoor characterization based on a graphite-coated and liquid nitrogen-cooled aluminum dome. Temperature tracking of a laminated pouch-coated (b) chip bag and (c) Ag mirror with stepwise increasing the solar light intensity via the indoor setup. (d) Steady-state temperature of the laminated pouch-coated chip bag and Ag mirror as a function of solar intensity. The straight lines indicate the linear fits to the data points. (e) Steady-state temperature for various samples measured with the indoor setup for both without (w/o) and with (w/) 100% solar light. The error bars correspond to the standard deviation of three different measurements.

increase in the foil thickness facilitates heat release, resulting in an increase in net cooling power in the nighttime. However, in the daytime, with the influence of the intensive solar light, the laminated pouch-coated Ag mirror decreased the net cooling power gradually by increasing the foil thickness. This is attributed to the larger amount of energy uptake from solar light caused by the foil thickness increase in comparison to the enhancement of heat release. By contrast, a minor influence is observed with laminated pouch-coated chip bags, arising from the less significant increase of the solar absorption of laminated pouch-coated chip bags (from 14.3 to 16.1%), with respect to that of the laminated pouch-coated Ag mirror (from 3.9 to 8.4%). The result observed here is in good agreement with the theoretical investigation of our previous work.²⁹ Based on the calculation, a pouch foil with a thickness of 80 μm possesses superior cooling performance among all tested thicknesses; it was thus used for the following studies.

APL Waste-Based Cooling Foil Characterization with the Indoor Setup. To experimentally demonstrate the passive cooling performance of the laminated pouch-based cooling devices, we first carried out the characterization with a homemade indoor setup. As shown in the schematic (Figure 3a), the indoor setup consists of an Al dome with its inner side coated with graphite to serve as a black-body absorber. During the measurement, the Al dome was cooled to about 80 K using liquid nitrogen, rendering it into a radiative heat sink. An AM 1.5 solar simulator illuminates the tested samples from the top, mimicking field testing during daytime conditions. The tunable solar intensity from the solar simulator enables us to thoroughly investigate the impact of solar light on cooling performance. In contrast, it is not possible for conventional field testing to determine the impact of a single parameter on the material cooling performance because of the time-varying weather conditions. More information about the indoor setup is presented in our previous work.³² For indoor characterization, we first measured the samples' steady-state temperature without

(w/o) solar light. A steady-state temperature of 12.0 and 13.9 $^{\circ}\text{C}$ was observed for a laminated pouch-coated chip bag and Ag mirror, respectively (Figure 3b–e). A subambient cooling of 8.1 and 6.2 $^{\circ}\text{C}$ was achieved with respect to the 'ambient temperature' (20.1 $^{\circ}\text{C}$), which is measured with a plain Ag mirror under identical measurement conditions without solar light. Despite that the subambient cooling is slightly overestimated by the indoor setup, which is caused by the absence of the atmospheric window, the decent nighttime cooling performance provided by both laminated pouch-based devices is verified. We observe a difference in the steady-state cooling temperature between the pouch-coated chip bag and the Ag mirror, despite their similar MIR absorption spectra. We attribute this deviation to the significant difference in the sample layout, about 200 μm for the pouch-coated chip bag sample and 3.2 mm for the pouch-coated Ag mirror, leading to a higher sample surface-to-thermocouple distance.³²

Subsequently, AM 1.5 solar light was illuminated onto the samples by a solar simulator to demonstrate the cooling performance during daytime. To reveal the impact of the solar light on the cooling performance, we stepwise increased the solar intensity from 0 to 25, 50, 75, and 100% of one-sun power (1000 W/m^2) after the sample's temperature reached a steady state. It must be noted that, based on our previous study, the intensity of the light reaching the sample is about 75% of the initial power due to the absorption, scattering, and reflection of the convection shield in the indoor setup.³² As shown in Figure 3b, after switching on the solar simulator, the temperature of the pouch-coated chip bag rose gradually until a steady state was reached, which is because of its solar absorption ($\sim 14\%$). Furthermore, the steady-state temperature increased linearly with the increase in solar intensity (Figure 3d). The pouch-coated chip bag reached a steady-state temperature of 16.9 $^{\circ}\text{C}$ with 100% solar illumination. By contrast, a less pronounced temperature rise is observed with the laminated pouch-coated Ag mirror due to its superior solar reflection ($\sim 96\%$). The

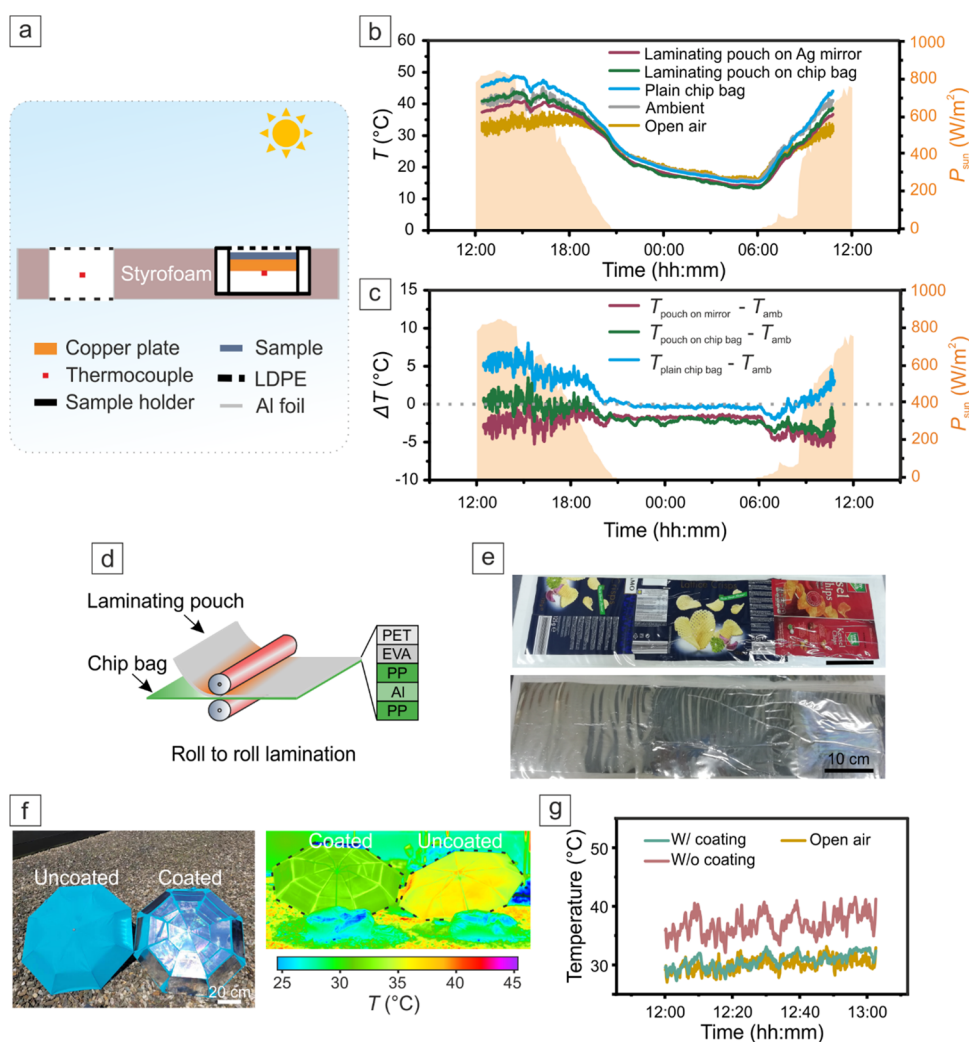


Figure 4. (a) Schematic of the homemade setup for field testing. The left thermocouple measures the ambient temperature, and the right thermocouple measures the sample temperature. (b) Temperature and (c) temperature difference for a laminated pouch-coated Ag mirror and chip bag. An untreated chip bag was measured as a reference, and the solar intensity was plotted as the background. The measurement was carried out under a clear sky on August 3rd, 2022, in Bayreuth, Germany. (d) Schematic of roll-to-roll lamination for large-scale passive daytime cooling foil fabrication. (e) Photography of fabricated chip bag-based cooling foil. (f) Photography and IR images of two common umbrellas. One is covered with fabricated cooling foil. (g) Temperature tracking under the two umbrellas. The measurement was performed under an average solar irradiation of 813 W/m^2 on August 11th, 2022, in Bayreuth, Germany.

pouch-coated Ag mirror reached a steady-state temperature of $15.8 \text{ }^\circ\text{C}$ with 100% solar illumination. Although 100% solar light caused a temperature rise of 4.9 and $1.9 \text{ }^\circ\text{C}$ for a pouch-coated chip bag and Ag mirror, a subambient cooling of 3.2 and $4.3 \text{ }^\circ\text{C}$ was observed, respectively, indicating the remarkable daytime cooling performance of the proposed cooling devices.

Another advantage of using the indoor setup to characterize the passive daytime cooling performance is that various cooling materials can be compared under identical measurement conditions. Using this advantage, we measured the steady-state temperature of a plain Ag mirror, chip bag, and graphite to further emphasize the daytime cooling performance of the laminated pouch-based cooling devices. The results are summarized in Figure 3e. It is clear that the laminated pouch foil greatly enhanced the cooling performance of both the untreated chip bag and Ag mirror by dramatically increasing the thermal radiation. Compared to graphite which possesses a high absorption in the solar and MIR range, laminated pouch-based cooling devices show a similar temperature in the dark case.

While in the light case, the graphite sample reached a much higher temperature due to the significant amount of solar absorption compared to the laminated pouch-based cooling devices. The temperature difference between the graphite sample and the pouch-coated Ag mirror and chip bag is 11.2 and $10.1 \text{ }^\circ\text{C}$, respectively. In addition, the temperature of the plain Ag mirror increased slightly under the solar light. We attributed this to the greenhouse effect caused by the parasitic solar light absorption of the Ag mirror and sample holder.³² Finally, the net cooling performance of pouch-coated chip bags with various pouch thicknesses was also determined via the indoor setup to confirm the numerical calculation. No pronounced difference in the steady-state temperature was observed between the pouch-coated chip bag with various thicknesses (Figure S8), verifying the simulation's prediction.

APL Waste-Based Cooling Foil Characterization with Field Testing. To further demonstrate the net cooling performance of the laminated pouch-based cooling devices, we conducted field testing under a clear sky in Bayreuth, Germany.

Figure 4a illustrates the schematic of the homemade setup for field testing. During the measurement, the samples were placed into a homemade sample holder surrounded by styrofoam to prevent undesired thermal conduction. Low-density polyethylene (LDPE) foil, which is highly transparent in both the solar and MIR range, is used to suppress convective heat transfer to the environment. Besides the laminated pouch-coated chip bag and Ag mirror, the temperature of ambient and open air and an untreated chip bag sample were also recorded during the test. The difference between the ambient and open-air temperature is caused by the enclosure of the ambient temperature thermocouple into a convection-shielded container, whereas the open-air temperature is exposed to wind. On account of the greenhouse effect, which was caused by parasitic solar absorption within the sample holder and the ambient measurement chamber, the temperature of all test samples and the ambient temperature were observed to be higher than in open air.²⁹ Figure 4b shows the recorded temperature of the tested samples for about 24 h, and Figure 4c shows the temperature difference between the tested samples and the ambient conditions. Even though the ambient temperature is higher compared to the open-air temperature, it represents a more suitable reference point for the samples' cooling performance since all of them are protected by an LDPE cover. The solar intensity was measured along with field testing and plotted as the background. Under an average solar irradiation of 838 W/m² (12:30–14:30), the average temperature difference to the ambient temperature was 5.6, 0.4, and –2.6 °C for the untreated chip bag, laminated pouch-coated chip bag, and laminated pouch-coated Ag mirror, respectively. The Al layer of the untreated chip bag is insufficient for passive cooling, even though it reflected a large amount of solar light (~86%). With a laminated pouch as an emittance enhancer, more heat was released via MIR radiation from the foil to outer space. Consequently, the laminated pouch exhibited a very similar temperature to that of the ambient, implying its satisfactory passive daytime cooling performance. Furthermore, the Ag mirror reflected most of the solar light (~96%), and the laminated pouch-coated Ag mirror thus achieved a subambient cooling of –2.6 °C. The temperature difference between the laminated pouch-coated chip bag and the Ag mirror relative to the ambient temperature amounts to –2.2 and –1.7 °C for the nighttime (22:00–05:00). Compared to the daytime, the cooling capacity of laminated pouch-coated Ag mirror was slightly reduced, which is likely attributed to the higher humidity at night.³³ The absolute humidity in air is shown in Figure S9.

Passive cooling foils constructed from the laminated pouch and chip bag are flexible, possess excellent mechanical strength, and, most importantly, can be easily fabricated with a common hot laminator (Figure 4d). Moreover, by carefully positioning the chip bag with respect to laminated pouch foil, several pieces of chip bag can be stitched together to form a large-scale cooling foil. Figure 4e illustrates a photograph of a fabricated cooling foil with three joined chip bags. The flexible cooling foil is ready to be used on any target surface to prevent overheating from the harsh solar light. To highlight this point, we attached the cooling foil to an umbrella with common double-sided adhesive tape, as shown in Figure 4f. To show the adequate protection of the cooling foil, the cooling foil-covered umbrella and a similar umbrella without cooling foil were placed under the sunlight. The IR image shows that the foil-covered umbrella exhibits a much lower temperature than the plain one. By measuring the temperature under each umbrella with a thermocouple, an

average temperature difference of 6.3 °C between 12:00 and 13:00 was observed between the cooling foil-covered and plain umbrella under an average solar irradiation of 813 W/m² (Figures 4g and S10). The much lower temperature achieved with a laminated pouch-coated chip bag indicates that it can effectively prevent the target object from overheating in hot climates and provide a comfortable temperature right beneath it. This exemplary use case indicates the potential of passive cooling materials for personal thermal comfort. Studies by Cui et al. have demonstrated how multilayered textiles can contribute to improved heat management based on functional apparel.^{34–36} Upcycled APLs (without a pouch) may serve as reflective layers in such apparel, lowering the ecological footprint of such commodity products.

Considering the energy-saving potentials on a larger scale, we conducted calculations based on EnergyPlus (Version 9.6.0)^{37–39} for mainland China. Comparing mid-rise buildings with and without passive cooling foils applied to the walls and roof, a clear energy saving on the order of tens of GJ can be expected across mainland China (Figure S11). The energy-saving effect depends on the geographic location. Compared to low-cost white paint, one particular advantage of the foils introduced here is their mechanical flexibility, allowing them to be folded or rolled up, making them attractive for applications complementary to wall or roof coatings. This renders them suitable for application to parasols and roller shutters, which introduces the possibility of turning the cooling performance on and off simply by rolling up or folding away the passive cooling device. This adjustability to actual weather conditions will be beneficial, for example, during cold winter days.

CONCLUSIONS

In this work, a processing strategy to upcycle the APL packaging waste to a valuable passive daytime cooling foil is outlined. By coupling the APL packing waste and a laminated pouch foil, a remarkably simple and low-cost but effective passive daytime cooling device is obtained, which exhibits satisfactory optical properties and, consequently, daytime cooling performance. The proposed APL waste-based cooling foil is flexible and scalable and can be readily applied to any target surface against harsh solar light in hot climates. More importantly, it is extremely easy to fabricate and can be constructed by every household with a common hot laminator. This simple technique can be applied worldwide, from which we expect significant contributions to comfortable temperature conditions during upcoming heat waves and surging urban heat island effects. Upcycling post-consumer plastic waste additionally reduces the ecological footprint of these plastic-based passive cooling materials.

ASSOCIATED CONTENT

Supporting Information

The Supporting Information is available free of charge at <https://pubs.acs.org/doi/10.1021/acssuschemeng.3c00683>.

Detailed information on the numerical calculations, microscope images of a laminating pouch, chemical and optical characterization of a laminating pouch, predicted cooling performance of a laminated pouch-coated Ag mirror, predicted cooling power and indoor characterization of laminating pouch-based cooling devices with different pouch thicknesses, and energy-saving prediction (PDF)

AUTHOR INFORMATION

Corresponding Authors

Qimeng Song – Department of Chemistry, Physical Chemistry I, University of Bayreuth, Bayreuth 95447, Germany; Email: qimeng.song@uni-bayreuth.de

Markus Retsch – Department of Chemistry, Physical Chemistry I and Bavarian Polymer Institute, Bayreuth Center for Colloids and Interfaces, and Bavarian Center for Battery Technology (BayBatt), University of Bayreuth, Bayreuth 95447, Germany; orcid.org/0000-0003-2629-8450; Email: markus.retsch@uni-bayreuth.de

Complete contact information is available at: <https://pubs.acs.org/10.1021/acssuschemeng.3c00683>

Notes

The authors declare no competing financial interest.

ACKNOWLEDGMENTS

The authors thank Stefan Rettinger and the mechanical workshop (University Bayreuth) for technical support. We gratefully thank Prof. Christoph Thomas for kindly providing the solar radiance and air temperature data. The authors acknowledge financial support from the European Research Council (ERC) under the European Union's Horizon 2020 research and innovation program (grant agreement no. 101082087).

REFERENCES

- (1) Association of Plastic Manufacturers. 2021. Plastics—The Facts. <https://plasticseurope.org/knowledge-hub/plastics-the-facts-2020/> (accessed Oct 6, 2022).
- (2) MacLeod, M.; Arp, H. P. H.; Tekman, M. B.; Jahnke, A. The global threat from plastic pollution. *Science* **2021**, *373*, 61–65.
- (3) Global Plastics Outlook. https://www.oecd-ilibrary.org/environment/data/global-plastic-outlook_c0821f81-en (accessed Oct 6, 2022).
- (4) Deshwal, G. K.; Panjagari, N. R. Review on metal packaging: materials, forms, food applications, safety and recyclability. *J. Food Sci. Technol.* **2020**, *57*, 2377–2392.
- (5) Bauer, A. S.; Tacker, M.; Uysal-Unalan, I.; Cruz, R. M. S.; Varzakas, T.; Krauter, V. Recyclability and redesign challenges in multilayer flexible food packaging—A review. *Foods* **2021**, *10*, 2702.
- (6) Lahme, V.; Daniel, R.; Marsh, P.; Molteno, S. Recycling of Multilayer Composite Packaging: the Beverage Carton, 2020. <https://zerowasteurope.eu/library/recycling-of-multilayer-composite-packaging-the-beverage-carton>.
- (7) Walker, T. W.; Frelka, N.; Shen, Z.; Chew, A. K.; Banick, J.; Grey, S.; Kim, M. S.; Dumesic, J. A.; Van Lehn, R. C.; Huber, G. W. Recycling of multilayer plastic packaging materials by solvent-targeted recovery and precipitation. *Sci. Adv.* **2020**, *6*, No. eaba7599.
- (8) Yin, S.; Rajarao, R.; Gong, B.; Wang, Y.; Kong, C.; Sahajwalla, V. Thermo-delamination of metallised composite plastic: An innovative approach to generate Aluminium from packaging plastic waste. *J. Cleaner Prod.* **2019**, *211*, 321–329.
- (9) Kremser, K.; Gerl, P.; Borrás, A. B.; Espinosa, D. R.; Martínez, B. M.; Guebitz, G. M.; Pellis, A. Bioleaching/enzyme-based recycling of aluminium and polyethylene from beverage cartons packaging waste. *Resour., Conserv. Recycl.* **2022**, *185*, No. 106444.
- (10) Ahamed, A.; Veksha, A.; Giannis, A.; Lisak, G. Flexible packaging plastic waste—environmental implications, management solutions, and the way forward. *Curr. Opin. Chem. Eng.* **2021**, *32*, No. 100684.
- (11) Farrukh, A.; Mathrani, S.; Sajjad, A. A systematic literature review on environmental sustainability issues of flexible packaging: potential pathways for academic research and managerial practice. *Sustainability* **2022**, *14*, 4737.
- (12) Santamouris, M.; Feng, J. Recent progress in daytime radiative cooling: is it the air conditioner of the future? *Buildings* **2018**, *8*, 168.
- (13) Zeyghami, M.; Goswami, D. Y.; Stefanakos, E. A review of clear sky radiative cooling developments and applications in renewable power systems and passive building cooling. *Sol. Energy Mater. Sol. Cells* **2018**, *178*, 115–128.
- (14) Zhao, B.; Hu, M.; Ao, X.; Chen, N.; Pei, G. Radiative cooling: A review of fundamentals, materials, applications, and prospects. *Appl. Energy* **2019**, *236*, 489–513.
- (15) Li, X.; Peoples, J.; Huang, Z.; Zhao, Z.; Qiu, J.; Ruan, X. Full Daytime Sub-ambient Radiative Cooling in Commercial-like Paints with High Figure of Merit. *Cell Rep. Phys. Sci.* **2020**, *1*, No. 100221.
- (16) Li, X.; Peoples, J.; Yao, P.; Ruan, X. Ultrawhite BaSO₄ Paints and Films for Remarkable Daytime Subambient Radiative Cooling. *ACS Appl. Mater. Interfaces* **2021**, *13*, 21733–21739.
- (17) Raman, A. P.; Anoma, M. A.; Zhu, L.; Rephaeli, E.; Fan, S. Passive radiative cooling below ambient air temperature under direct sunlight. *Nature* **2014**, *515*, 540–544.
- (18) Chae, D.; Kim, M.; Jung, P. H.; Son, S.; Seo, J.; Liu, Y.; Lee, B. J.; Lee, H. Spectrally selective inorganic-based multilayer emitter for daytime radiative cooling. *ACS Appl. Mater. Interfaces* **2020**, *12*, 8073–8081.
- (19) Mandal, J.; Fu, Y.; Overvig, A. C.; Jia, M.; Sun, K.; Shi, N. N.; Zhou, H.; Xiao, X.; Yu, N.; Yang, Y. Hierarchically porous polymer coatings for highly efficient passive daytime radiative cooling. *Science* **2018**, *362*, 315–319.
- (20) Liu, X.; Zhang, M.; Hou, Y.; Pan, Y.; Liu, C.; Shen, C. Hierarchically superhydrophobic stereo-complex poly (lactic acid) aerogel for daytime radiative cooling. *Adv. Funct. Mater.* **2022**, *32*, No. 2207414.
- (21) Wang, T.; Wu, Y.; Shi, L.; Hu, X.; Chen, M.; Wu, L. A structural polymer for highly efficient all-day passive radiative cooling. *Nat. Commun.* **2021**, *12*, No. 365.
- (22) Zhai, Y.; Ma, Y.; David, S. N.; Zhao, D.; Lou, R.; Tan, G.; Yang, R.; Yin, X. Scalable-manufactured randomized glass-polymer hybrid metamaterial for daytime radiative cooling. *Science* **2017**, *355*, 1062–1066.
- (23) Bao, H.; Yan, C.; Wang, B.; Fang, X.; Zhao, C. Y.; Ruan, X. Double-layer nanoparticle-based coatings for efficient terrestrial radiative cooling. *Sol. Energy Mater. Sol. Cells* **2017**, *168*, 78–84.
- (24) Zhou, L.; Song, H.; Liang, J.; Singer, M.; Zhou, M.; Stegenburgs, E.; Zhang, N.; Xu, C.; Ng, T.; Yu, Z.; Ooi, B.; Gan, Q. A polydimethylsiloxane-coated metal structure for all-day radiative cooling. *Nat. Sustainability* **2019**, *2*, 718–724.
- (25) Lin, K.; Chao, L.; Ho, T. C.; Lin, C.; Chen, S.; Du, Y.; Huang, B.; Tso, C. Y. A flexible and scalable solution for daytime passive radiative cooling using polymer sheets. *Energy Build.* **2021**, *252*, No. 111400.
- (26) Mieth, A.; Hoekstra, E.; Simoneau, C. *Guidance for the Identification of Polymers in Multilayer Films Used in Food Contact Materials: User Guide of Selected Practices to Determine the Nature of Layers*, EUR 27816; Publications Office of the European Union, 2016.
- (27) Jiang, Z.; Hu, C.; Easa, S. M.; Zheng, X.; Zhang, Y. Evaluation of physical, rheological, and structural properties of vulcanized EVA/SBS modified bitumen. *J. Appl. Polym. Sci.* **2017**, *134*, 44850.
- (28) Pereira, A. P. d. S.; Silva, M. H. P. d.; Lima Júnior, É. P.; Paula, A. d. S.; Tommasini, F. J. Processing and characterization of pet composites reinforced with geopolymer concrete waste. *Mater. Res.* **2017**, *20*, 411–420.
- (29) Herrmann, K.; Lauster, T.; Song, Q.; Retsch, M. Homogeneous Polymer Films for Passive Daytime Cooling: Optimized Thickness for Maximized Cooling Performance. *Adv. Energy Sustainability Res.* **2021**, *3*, No. 2100166.
- (30) Solar Spectral Irradiance: Air Mass 1.5. <http://redc.nrel.gov/solar/spectra/am1.5> (accessed Jun 15, 2022).
- (31) Spectral Atmospheric Transmittance. <https://www.gemini.edu/observing/telescopes-and-sites/sites#Transmission> (accessed Jun 15, 2022).

(32) Song, Q.; Tran, T.; Herrmann, K.; Lauster, T.; Breitenbach, M.; Retsch, M. A tailored indoor setup for reproducible passive daytime cooling characterization. *Cell Rep. Phys. Sci.* **2022**, *3*, No. 100986.

(33) Jaramillo-Fernandez, J.; Yang, H.; Schertel, L.; Whitworth, G. L.; Garcia, P. D.; Vignolini, S.; Sotomayor-Torres, C. M. Highly-Scattering Cellulose-Based Films for Radiative Cooling. *Adv. Sci.* **2022**, *9*, No. e2104758.

(34) Peng, Y.; Chen, J.; Song, A. Y.; Catrysse, P. B.; Hsu, P.-C.; Cai, L.; Liu, B.; Zhu, Y.; Zhou, G.; Wu, D. S.; Lee, H. R.; Fan, S.; Cui, Y. Nanoporous polyethylene microfibrils for large-scale radiative cooling fabric. *Nat. Sustainability* **2018**, *1*, 105–112.

(35) Hsu, P. C.; Liu, C.; Song, A. Y.; Zhang, Z.; Peng, Y.; Xie, J.; Liu, K.; Wu, C. L.; Catrysse, P. B.; Cai, L.; Zhai, S.; Majumdar, A.; Fan, S.; Cui, Y. A dual-mode textile for human body radiative heating and cooling. *Sci. Adv.* **2017**, *3*, No. e1700895.

(36) Cai, L.; Song, A. Y.; Wu, P.; Hsu, P. C.; Peng, Y.; Chen, J.; Liu, C.; Catrysse, P. B.; Liu, Y.; Yang, A.; Zhou, C.; Zhou, C.; Fan, S.; Cui, Y. Warming up human body by nanoporous metallized polyethylene textile. *Nat. Commun.* **2017**, *8*, No. 496.

(37) Li, X.; Sun, B.; Sui, C.; Nandi, A.; Fang, H.; Peng, Y.; Tan, G.; Hsu, P. C. Integration of daytime radiative cooling and solar heating for year-round energy saving in buildings. *Nat. Commun.* **2020**, *11*, No. 6101.

(38) Peng, Y. C.; Fan, L. L.; Jin, W. L.; Ye, Y. S.; Huang, Z. J.; Zhai, S.; Luo, X.; Ma, Y. X.; Tang, J.; Zhou, J. W.; Greenburg, L. C.; Majumdar, A.; Fan, S. H.; Cui, Y. Coloured low-emissivity films for building envelopes for year-round energy savings. *Nat. Sustainability* **2022**, *5*, 339–347.

(39) Wang, S.; Jiang, T.; Meng, Y.; Yang, R.; Tan, G.; Long, Y. Scalable thermochromic smart windows with passive radiative cooling regulation. *Science* **2021**, *374*, 1501–1504.